PHILOSOPHICAL MAGAZINE LETTERS, 1999, VOL. 79, NO. 10, 785–796

Dislocation density evolution upon plastic deformation of Al–Pd–Mn single quasicrystals

P. SCHALL†, M. FEUERBACHER†§, M. BARTSCH‡, U. MESSERSCHMIDT‡ and K. URBAN†

† Institut für Festkörperforschung, Forschungszentrum Jülich GmbH, D-52425 Jülich, Germany
‡ Max-Planck-Institut für Mikrostrukturphysik, D-06120 Halle/Saale, Germany

[*Received 14 April 1999 and accepted 21 June 1999*]

ABSTRACT

Dislocation density studies have been performed on icosahedral Al–Pd–Mn single quasicrystals after plastic deformation and after subsequent heat treatment. The deformation tests were carried out at a constant strain rate of $10^{-5}\,s^{-1}$ at temperatures between 695 and 820°C. The heat treatments were performed at 730°C, corresponding to one of the deformation temperatures. The development of the dislocation density during heat treatment and that during plastic deformation are compared. The experimental data are interpreted using a kinetic equation, which describes the evolution of the dislocation density during deformation. Numerical values for the dislocation multiplication constant and the annihilation rate for icosahedral Al–Pd–Mn are presented.

§ 1. INTRODUCTION

In many respects, quasicrystals show plastic properties which are unusual in comparison with crystalline materials, especially metals. They are brittle at room temperature but at elevated temperatures they show extensive ductile behaviour. The brittle-to-ductile transition occurs at very high temperatures of about 80% (at a strain rate of $10^{-5}\,s^{-1}$) of the melting temperature. The most prominent feature of the plastic behaviour is the absence of a work-hardening regime at higher strains.

The plastic properties of quasicrystals have mostly been investigated on icosahedral Al–Pd–Mn, which can be grown in the form of large single quasicrystals of high structural quality by means of the Czochralski technique (Yokoyama *et al.* 1992). It has been shown that the plastic deformation mechanism is mediated by the motion of dislocations (Wollgarten *et al.* 1993, 1995). The plastic behaviour can be described in terms of a thermally activated mechanism; the thermodynamic activation parameters have been determined by Feuerbacher *et al.* (1995) and Geyer *et al.* (2000) and have been discussed by Messerschmidt *et al.* (1999). Rosenfeld *et al.* (1995) and Feuerbacher *et al.* (1997) performed microstructural analyses on deformed icosahedral Al–Pd–Mn quasicrystals, including the determination of dislocation densities, Burgers vectors and slip systems.

In order to understand the deformation process it is important to have detailed knowledge about the evolution of the dislocation structure as a function of plastic

§ Email: m.feuerbacher@fz-juelich.de.

Philosophical Magazine Letters ISSN 0950–0839 print/ISSN 1362–3036 online
http://www.tandf.co.uk/JNLS/phl.htm
http://www.taylorandfrancis.com/JNLS/phl.htm

strain and deformation temperature. Since the deformation tests have to be carried out at very high temperatures, recovery effects influencing the deformation behaviour cannot be excluded. In this paper we present a detailed study of dislocation densities in plastically deformed Al–Pd–Mn quasicrystals, providing a data set of dislocation densities as a function of plastic strain and deformation temperature. In addition, we present the results of heat treatments on deformed samples, which have been carried out at temperatures equal to those of the deformation tests.

§ 2. Experimental details

Rectangular samples of about 7 mm × 2 mm × 2 mm, with surfaces oriented perpendicular to twofold directions, were cut from a Czochralski-grown single quasicrystal. Deformation tests in compression along the longitudinal axis were performed using an INSTRON 8562 mechanical testing system at a constant strain rate of $10^{-5}\,s^{-1}$. In a first deformation series, samples were deformed at the temperature T = 730°C up to various plastic strains ε_{plast} = 0.1, 0.3, 0.5, 1.5, 3.8, 5.2, 8.2 and 11.1%. Additional deformation tests were carried out at the temperatures T = 695, 790 and 820°C up to equal deformation stages. After each deformation test the samples were rapidly unloaded and quenched in water within less than 1 min.

The deformed samples were cut into slices of 0.4 mm thickness perpendicular to the deformation axis. From each sample, the slice positioned at about one third of the total length was prepared for investigations in a transmission electron microscope by mechanical grinding and subsequent argon-ion milling. The microstructural analyses of these specimens were carried out in JEOL 4000 FX and 2000 EX microscopes operated at 200 kV.

In order to investigate the annealing behaviour of the microstructure of the deformed material, heat treatments were performed on slices of the deformed samples. A series with different annealing times was performed on slices of the sample deformed at 730°C by ε_{plast} = 5.2%, which were positioned next to the slice investigated in the as-deformed state. For this, the slices were annealed at 730°C for 13, 45 and 90 min and subsequently quenched in water. Additionally, slices of two other samples deformed up to ε_{plast} = 1.5 and 8.2% were heated at 730°C for 45 min. After the heat treatment, the slices were prepared for investigations in the transmission electron microscope as described above.

To determine the dislocation density, about 20 bright-field images were taken under two-beam conditions at different positions of a specimen at a magnification of about 20 000. The dislocation density was determined from the micrographs by counting the intersections of the dislocations with the specimen surfaces. With N denoting the number of intersections of dislocations with both surfaces of the specimen, the dislocation density can be calculated from (Ham and Sharpe 1961)

$$\rho = N/a, \qquad (1)$$

where a is the area of the sample region examined.

§ 3. Results

Figure 1 (*a*) shows true stress–true strain curves of the deformation tests performed at 730°C. The full circles mark the end of each deformation test. The curves of the different deformation tests show good coincidence. We observe a pronounced yield drop of about 15% of the upper yield stress which amounts to about 400 MPa. After the yield drop the stress continuously decreases with increasing strain.

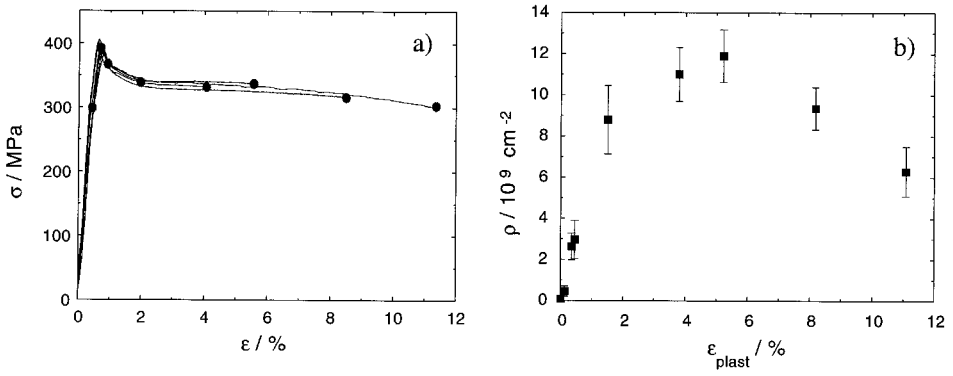

Figure 1. (*a*) True stress–true strain curves of icosahedral Al–Pd–Mn at $T = 730°C$ and a strain rate $10^{-5}\,s^{-1}$: (●), the end of each deformation test. (*b*) Dislocation density ρ as a function of plastic strain ε_{plast} at $T = 730°C$.

The dislocation density ρ of the deformed samples is plotted in figure 1(*b*) as a function of plastic strain ε_{plast}. The error bars indicate the statistical error. At the onset of plastic deformation the dislocation density increases approximately linearly with increasing strain. Then further nonlinear growth up to $\rho = 12 \times 10^9\,cm^{-2}$ at $\varepsilon_{plast} = 5.2\%$ followed by a subsequent decrease down to about 50% of the maximum dislocation density is observed. A linear regression through the first five data points yields a slope of

$$\left(\frac{d\rho}{d\varepsilon}\right)_M \equiv M = 6.5 \times 10^{11}\,cm^{-2}, \qquad (2)$$

which is the multiplication constant M of the dislocation density.

Figure 2(*a*) shows true stress–true strain curves of the deformation tests at the temperatures $T = 695$, 730, 790 and 820°C. The flow stress at the upper yield point decreases from 560 MPa for the deformation at $T = 695°C$ to 97 MPa at $T = 820°C$.

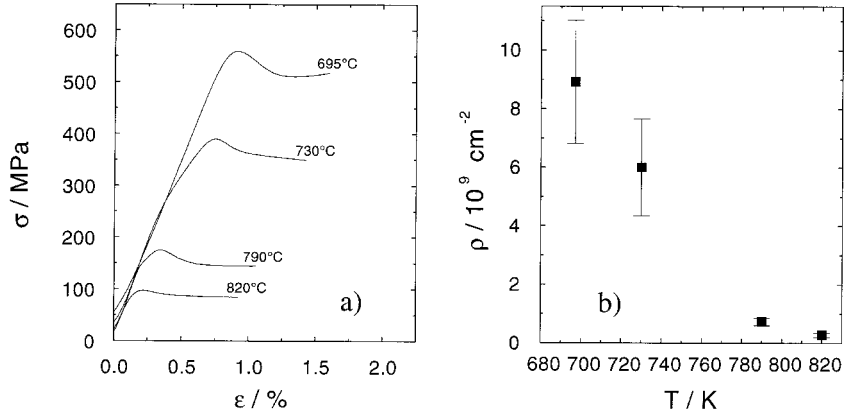

Figure 2. (*a*) True stress–true strain curves of icosahedral Al–Pd–Mn at $T = 695$, 730, 790 and 820°C and a strain rate of $10^{-5}\,s^{-1}$. (*b*) Dislocation density ρ as a function of temperature.

Figure 3. Bright-field electron micrograph of the sample deformed by $\varepsilon_{plast} = 5.2\%$; (*a*) as deformed; (*b*) after heat treatment for 13 min at 730°C; (*c*) after heat treatment for 90 min at 730°C.

The yield drop amounts to 8–15% of the maximum flow stress and decreases with increasing temperature. The ends of the deformation curves, which are at equal deformation stages, shift to smaller total strain ε with increasing temperature because of the decreasing amount of elastic strain. In the different deformation tests the upper yield point is observed at strains $\varepsilon = 0.9$, 0.75, 0.34 and 0.22% at $T = 695$, 730, 790 and 820°C respectively. The dislocation densities at the final stage of the deformation tests, that is in the deformed and quenched samples, are depicted in figure 2(*b*). A decrease in the dislocation density by two orders of magnitude between the deformations at $T = 695$ and 820°C is found.

Figure 3(*a*) shows a typical bright-field electron micrograph of the sample deformed at 730°C by $\varepsilon_{plast} = 5.2\%$, which shows the highest deformation-induced dislocation density. Figures 3(*b*) and (*c*) show typical examples of the dislocation arrangement in material from the same deformation sample subjected to subsequent heat treatments of 13 and 90 min respectively, at 730°C. Obviously, the dislocation density significantly decreases during the heat treatment. No polygonization or rearrangement of the dislocations in cell structures has been observed. A quantitative analysis of the dislocation density evolution upon annealing was carried out, the results of which are depicted in figure 4. In figure 4(*a*) the dislocation density in the sample deformed by $\varepsilon_{plast} = 5.2\%$ at 730°C is plotted as a function of annealing time. The first data point refers to the as-deformed sample. A first rapid drop is followed by a saturation at annealing durations exceeding about 40 min. During heat treatment for about 45 min the dislocation density decreases to about one third of the value of the untreated material. The slope at the beginning of the heat treatment amounts to $6.7 \times 10^6\ cm^{-2}\ s^{-1}$.

Figure 4(*b*) shows the result of the heat treatments of equal duration performed on samples deformed up to different strains. The full circles depict the plastic strain dependence of the dislocation density in the as-deformed samples as plotted in figure 1(*b*). The dislocation densities determined after annealing for 45 min at 730°C at plastic strains of 1.5, 5.2 and 8.2% are represented by the full squares with error bars. No significant dependence of the dislocation density reduction on the deformation stage can be observed. In each case a heat treatment of 45 min leads to a

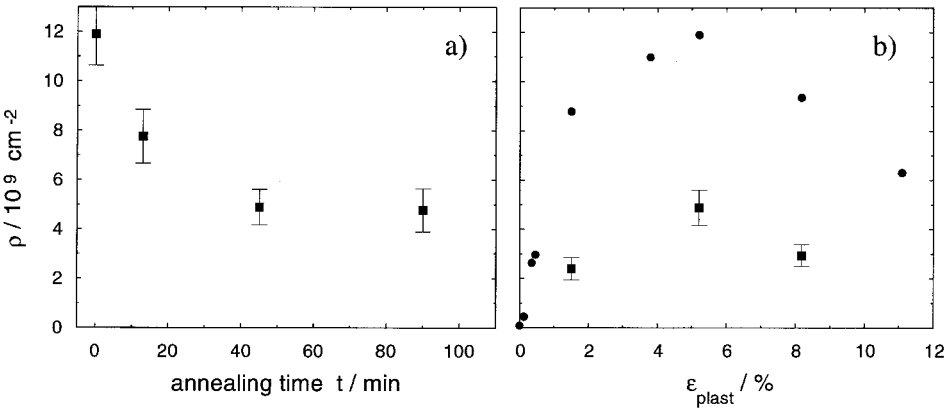

Figure 4. (*a*) Dislocation density ρ in deformed icosahedral Al–Pd–Mn ($\varepsilon_{plast} = 5.2\%$; $T = 730^{\circ}C$) as a function of annealing time t. (*b*) Dislocation density ρ as a function of plastic strain after deformation (●) and after deformation and subsequent heat treatment at $T = 730^{\circ}C$ for 45 min (■).

decrease in dislocation density down to about 30–40% with respect to the as-deformed samples.

§ 4. Discussion

In this paper we provide experimental data on the development of the dislocation density during plastic deformation and subsequent heat treatment. The strain dependence of the dislocation density (figure 1(*b*)) shows a rapid increase at the onset of plastic deformation up to a maximum value, followed by a significant decrease at higher strains. The latter behaviour distinctly differs from that of crystalline materials, where the total dislocation density in most cases is found to increase monotonically with increasing strain. The observed dependence of the dislocation density on strain can be compared with earlier studies on the same material. Feuerbacher *et al.* (1997) performed deformation tests at $T = 760^{\circ}C$ and observed a dislocation density evolution showing the same characteristics as in the present study (figure 2(*b*)). These workers used an incorrect equation for the dislocation density, leading to values too small by a factor of two. A re-evaluation using the correct equation (1) leads to a maximum value of $3.6 \times 10^{9}\,cm^{-2}$ which fits well the values observed in the present study (figure 2(*b*)). Rosenfeld *et al.* (1995) studied the dislocation density of samples deformed up to 2% plastic strain at different temperatures. After deformation the samples were cooled in the testing machine at a rate of about $12^{\circ}C\,min^{-1}$. At 730°C these workers found a dislocation density $\rho = 0.8 \times 10^{9}\,cm^{-2}$, also using the incorrect equation to determine the dislocation density. The corrected value amounts to $1.6 \times 10^{9}\,cm^{-2}$, which is comparable with the dislocation density observed in the sample deformed up to 1.5% plastic strain and annealed for 45 min at 730°C in the present study. This comparison shows that the dislocation density is reduced during the slow cooling process after the deformation.

In the present study, the samples were quenched in water within less than 1 min after unloading. Nevertheless, relaxation processes taking place within the time interval after unloading and before quenching still lead to a systematic error in

the determination of the dislocation density. Considering the initial slope of the $\rho(t)$ curve (figure 4(*a*)) this error can be estimated. A time interval of 1 min before quenching corresponds to a reduction in the dislocation density of $0.4 \times 10^9\ \mathrm{cm}^{-2}$, which is about 3% of the measured value. This systematic error can thus be neglected.

The linear increase in the dislocation density at the early stage of deformation has also been observed in crystalline materials. Reid *et al.* (1965), comparing the dislocation density evolution of about 20 different crystalline materials at the onset of plastic deformation, found a phenomenological multiplication law of the form $\rho = \rho_0 + M'\varepsilon^{\beta}$, where ρ_0 is the initial dislocation density and the exponent β is a constant taking on values between 0.5 and 2, most frequently close to unity. They found that the multiplication constant M' does not depend on the strain rate or temperature but increases systematically with increasing initial dislocation density ρ_0. According to their values, an initial dislocation density ρ_0 of $8 \times 10^7\ \mathrm{cm}^{-2}$, as observed in the present study, corresponds to a multiplication constant of the order of $10^{11}\ \mathrm{cm}^{-2}$. The multiplication constant (2) measured in the present study, which corresponds to the case $\beta = 1$, is larger by a factor of about six but lies within the spread of the data points obtained by Reid *et al.* (1965).

The yield drop in the stress–strain curves can be quantitatively accounted for by the corresponding increase in the dislocation density, that is the difference $\Delta\rho = \rho_{\mathrm{lyp}} - \rho_{\mathrm{uyp}}$ between the dislocation density in samples quenched at the upper yield point and the dislocation density in samples quenched at the lower yield point. Consider the Orowan equation (Kocks *et al.* 1975)

$$\dot{\varepsilon}_{\mathrm{plast}} = \rho_{\mathrm{m}} b v \tag{3}$$

(ρ_{m} denotes the density of mobile dislocations, b the modulus of the Burgers vector and v the mean glide velocity of the dislocations) and a dependence of v on the effective shear stress τ_{eff} in the glide plane of the form (Johnston 1962)

$$v \propto \tau_{\mathrm{eff}}^{m}, \tag{4}$$

where m is the stress exponent. τ_{eff} is related to the stress in the glide plane τ by

$$\tau_{\mathrm{eff}} = \tau - \tau_{\mathrm{i}} \tag{5}$$

(Seeger 1958). The long-range internal stress τ_{i} is given by (Taylor 1934)

$$\tau_{\mathrm{i}} = \alpha \mu b \rho^{1/2}. \tag{6}$$

The numerical constant α is typically in the range 0.2–0.5. μ is the shear modulus. The applied stress σ is related to τ by $\tau = m_{\mathrm{s}}\sigma$, where m_{S} is the Schmid factor.

At the upper and lower yield points we have $\dot{\sigma} = 0$, that is the plastic strain rate $\dot{\varepsilon}_{\mathrm{plast}}$ is given by the strain rate of the testing machine of $10^{-5}\ \mathrm{s}^{-1}$. According to equations (3) and (4) the ratio of the effective stresses at the upper and lower yield point is then given by

$$\frac{\tau_{\mathrm{eff,uyp}}}{\tau_{\mathrm{eff,lyp}}} = \left(\frac{\rho_{\mathrm{lyp}}}{\rho_{\mathrm{uyp}}}\right)^{1/m}. \tag{7}$$

Inserting the values $\alpha = 0.3$, $\mu = 70\ \mathrm{GPa}$ (Feuerbacher *et al.* 1996), $m = 4$ (Feuerbacher *et al.* 1995), $m_{\mathrm{S}} = 0.4$ and $b = 0.183\ \mathrm{nm}$ (Rosenfeld *et al.* 1995), a decrease $\Delta\sigma$ in the flow stress of 50 MPa is obtained as a result of the increase in

the dislocation density from $\rho_{uyp} = 2.6 \times 10^9\,cm^{-2}$ at the upper yield point to $\rho_{lyp} = 8.8 \times 10^9\,cm^{-2}$ at the lower yield point.

This value is in good agreement with the experimentally observed drop $\Delta\sigma$ in the flow stress of 55 MPa (figure 1(*a*)). Note that we have inserted the experimentally determined total dislocation density in our calculations, implying the assumption of $\rho \approx \rho_m$, where ρ_m denotes the mobile dislocation density, for our material. This is justified by the observation that, in our samples, the dislocations are homogeneously distributed. No arrangements in densely entangled networks are observed. Therefore, in a first approximation all dislocations are assumed to be mobile.

The behaviour at the yield point, described by equations (3)–(7), that is a stress drop accompanied by an increase in the mobile dislocation density, is well known from crystalline materials (Johnston 1962, Alexander and Haasen 1968). In crystals at higher strains the density of dislocations increases, which leads (equation (6)) to an increase in the internal stress. This is the well known work-hardening behaviour. Although in the present study the behaviour at the yield drop is in accordance with equations (3)–(7), at higher strains a behaviour different from that in crystals is found. Here, a decrease in the flow stress is accompanied by a significant decrease in dislocation density. This decrease in dislocation density leads to a decrease in the internal stress, which can be calculated according to equation (6). With the observed dislocation density decrease $\Delta\rho' = 5.7 \times 10^9\,cm^{-2}$ between the values at 5.2 and 11.1% plastic strain, a difference in internal stress of 11.7 MPa follows. For this calculation we have used the same values for α, b and μ as for the calculation of the yield drop. The observed decrease $\Delta\sigma'$ in the flow stress over the same strain interval amounts to 30.1 MPa, corresponding to $\Delta\tau' = 12.0$ MPa with $m_S = 0.4$.

The equality of these values shows that the decrease in the internal stress can account for the observed decrease in the flow stress. Thus (equation (1)) we can conclude that the effective stress is constant in this strain regime. Then, according to equation (4), the dislocation velocity should be constant and, with equation (3), the dislocation density should also be constant at the given constant strain rate. This is not in agreement with the experimental observation of a decreasing dislocation density. This contradiction can be solved by assuming that during plastic deformation the structure of the material is changed. The decrease in dislocation density has to be compensated by an increase in dislocation velocity, that is the structure of the material changes towards a structure of higher dislocation mobility.

This conclusion is in agreement with previous electron diffraction experiments on deformed Al–Pd–Mn quasicrystals by Franz *et al.* (1999). These workers found direct evidence for the accumulative introduction of phason defects into the material in the course of plastic deformation. The cluster friction model (Feuerbacher *et al.* 1997), which qualitatively describes the plastic deformation of icosahedral quasicrystals, also contains deformation-induced structure changes as a central ingredient. In this model, the Mackay-type clusters, which are the elementary building blocks of the icosahedral structure, are assumed to act as rate-controlling obstacles to dislocation motion. The net density of clusters is reduced by moving dislocations introducing disorder into the structure. This structure change leads to an increased dislocation mobility.

At a strain rate of $10^{-5}\,s^{-1}$ deformation from $\varepsilon_{plast} = 5.2\%$ to $\varepsilon_{plast} = 11.2\%$, that is the strain interval in which the dislocation density decreases, takes about 100 min. Within this time interval the dislocation density is reduced to about 50%

of its maximum value. Annealing at 730°C for 40 min after deformation by 5.2% at the same temperature leads to a reduction to about 40% of the original maximum value (figure 4(*a*)). Thus, the decrease in the dislocation density at higher strains can be accounted for by the annihilation processes taking place during the deformation. The difference between the two values shows that, at high strains, dislocation sources are still active, maintaining the dislocation density necessary for deformation at the given strain rate and structure.

The development of the dislocation density upon annealing as depicted in figure 4(*a*) is typical of a recovery process as observed in crystalline materials (for example Gottstein (1998)). At short annealing times, a high rate of dislocation density reduction is observed which, after a longer annealing duration, develops into a saturation behaviour. The rate of reduction in the dislocation density at the beginning of a heat treatment, that is the initial slope of the annealing-time dependence (figure 4(*a*)), amounts to $(\mathrm{d}\rho/\mathrm{d}t)_A = 6.7 \times 10^6\,\mathrm{cm}^{-2}\,\mathrm{s}^{-1}$. This means that a considerable number of dislocations are annihilated on a time scale of some minutes. Within 10 min, for example, the dislocation density at 730°C decreases by 30% of the maximum value. This shows that stress relaxation or temperature-change experiments, which are conducted during time intervals of this magnitude, can be considerably influenced by recovery effects. This has been discussed by Messerschmidt *et al.* (1999).

The elementary mechanism of static recovery in crystals is the annihilation of two dislocations of opposite signs approaching each other owing to their attractive interaction. The probability of finding two dislocations of opposite signs within a distance small enough for annihilation is proportional to the square of the dislocation density. Thus,

$$\left(\frac{\mathrm{d}\rho}{\mathrm{d}t}\right)_A = -A\rho^2, \tag{8}$$

where A is a constant at a given temperature (for example Ilschner (1966) and Li (1966)). Integration of equation (8) yields

$$\frac{1}{\rho} = At + B, \tag{9}$$

where B is a constant.

As depicted in figure 5 the initial decrease in the dislocation density can be well described in terms of static recovery (equation (9)) whereas the behaviour for longer annealing times deviates from this behaviour. A linear regression of the first three data points yields

$$A = 4.63 \times 10^{-14}\,\mathrm{cm}^2\,\mathrm{s}^{-1}, \quad B = 0.085\,\mathrm{cm}^2. \tag{10}$$

The annihilation rate and the multiplication constant can be combined to give a kinetic rate equation balancing the dislocation density during deformation. The net rate of the variation in the dislocation density with time results from the difference between a creation rate $(\mathrm{d}\rho/\mathrm{d}t)_M$ due to multiplication and a loss rate $(\mathrm{d}\rho/\mathrm{d}t)_A$ due to annihilation processes:

$$\frac{\mathrm{d}\rho}{\mathrm{d}t} = \left(\frac{\mathrm{d}\rho}{\mathrm{d}t}\right)_M - \left(\frac{\mathrm{d}\rho}{\mathrm{d}t}\right)_A. \tag{11}$$

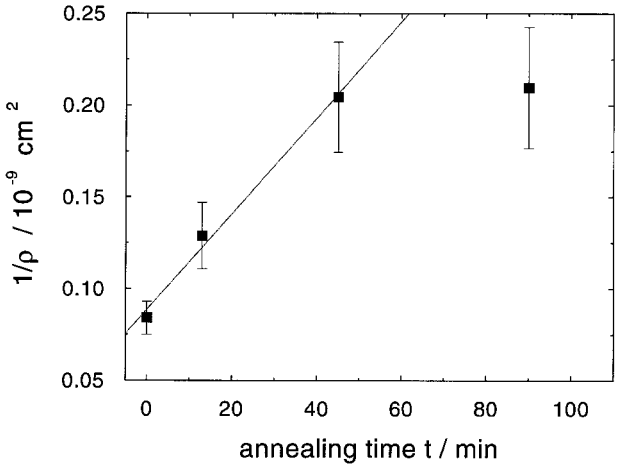

Figure 5. Reciprocal dislocation density $1/\rho$ as a function of annealing time t. The line is a linear fit of the first three data points.

Assuming static recovery, the annihilation rate during deformation is given by equation (8). The dislocation multiplication can be described by a model developed by Johnston and Gilman (1959). They assumed that an expanding dislocation loop leaves a trail containing δ new dislocations per unit length moved. The length $d\rho$ of new dislocations per volume, that is the dislocation density produced during a movement of ds, then amounts to

$$d\rho = 2\delta\rho\, ds. \tag{12}$$

Peissker *et al.* (1962) proposed that δ has a stress dependence of the form

$$\delta = c\tau_{eff}^{n}, \tag{13}$$

where c and n are constants. For the present case we set $n = 1$ (Peissker *et al.* 1962). With $d\varepsilon = \rho b\, ds$ we arrive at the expression

$$\left(\frac{d\rho}{d\varepsilon}\right)_M = \frac{2c}{b}\tau_{eff} = M \tag{14}$$

for the multiplication constant M. With $d\varepsilon = \dot{\varepsilon}\, dt$, equation (11) can then be written as

$$\frac{d\rho}{d\varepsilon} = M - \frac{A}{\dot{\varepsilon}}\rho^2, \tag{15}$$

where we can enter the experimental values $M = 6.5 \times 10^{11}\,cm^{-2}$ and $A = 4.63 \times 10^{-14}\,cm^2\,s^{-1}$ for the strain rate $\dot{\varepsilon} = 10^{-5}\,s^{-1}$. Equation (15) describes a saturation of the dislocation density at a steady state value ρ_{ss} defined by $(d\rho/d\varepsilon)|_{\rho_{ss}} = 0$:

$$\rho_{ss} = \left(\frac{\dot{\varepsilon}M}{A}\right)^{1/2}. \tag{16}$$

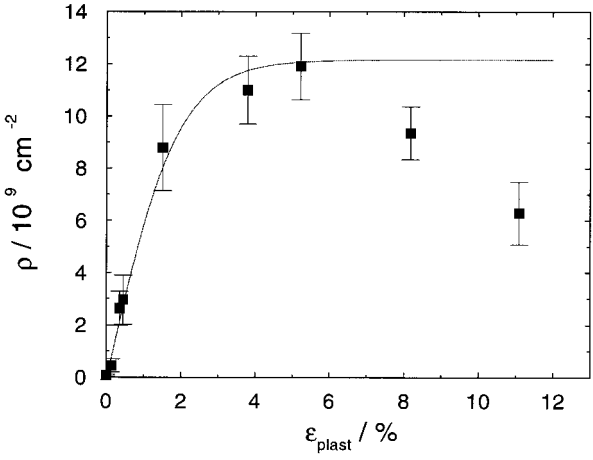

Figure 6. Dislocation density evolution calculated according to the kinetic equation (15) (——) and experimental values (■).

With the experimental values for A and M (equations (10) and (2)) we find that $\rho_{ss} = 12.1 \times 10^9\ cm^{-2}$, in very good agreement with the experimental maximum value of ρ. Figure 6 shows the development of the dislocation density calculated according to equation (15) using the values determined for A and M in comparison with the experimental values of the dislocation density as given in figure 1 (*b*). Up to a plastic strain of about 5% the calculated dislocation density shows good agreement with the experimental values, whereas the saturation behaviour in the second part deviates significantly from the measured dislocation density. The saturating behaviour as described by equation (15) is observed in many crystalline materials. At low temperatures the mobile dislocation density saturates whereas the density of immobilized dislocations monotonically increases (for example Gillis and Gilman (1965) and Alexander and Haasen (1968)). The loss term in the kinetic equation formulated for the mobile dislocation density is then given by immobilization mostly due to dislocation interactions. At high temperatures the total dislocation density saturates since annihilation processes determine the loss term in equation (11) (Gillis and Gilman 1965).

The decrease in dislocation density occurring at higher strains can be understood as a result of structural changes in the material due to moving dislocations as discussed above. These structural changes are not accounted for in the kinetic equation (15). In terms of the steady-state dislocation density ρ_{ss}, the dislocation densities measured at high strains are values of a dynamic equilibrium in a succession of steady states belonging to different structural states.

The temperature dependence of the dislocation density (figure 2 (*b*)) can be interpreted in terms of an Arrhenius *Ansatz*. Assuming that the annihilation rate A of equation (8) for the static recovery is proportional to an exponential term containing the activation enthalpy of H_{SD} of self-diffusion (Alden 1969, Nordstrom and Barrett 1972):

$$A \propto \exp\left(-\frac{H_{SD}}{kT}\right), \tag{17}$$

we obtain with equations (14) and (16)

$$\ln\left(\frac{\tau_{\mathrm{eff}}}{\rho_{\mathrm{ss}}^2}\right) = \text{constant} - \frac{H_{SD}}{kT}, \qquad (18)$$

with τ_{eff} according to equation (5). In a logarithmic representation of the values $\tau_{\mathrm{eff}}/\rho_{\mathrm{ss}}^2$ as a function of $1/kT$ the data points can be fitted by a straight line with a slope of $H_{SD} \approx 3.9 \pm 0.6\,\mathrm{eV}$. This value is considerably larger than the diffusion enthalpy of 2.32 eV for palladium (Blüher *et al.* 1998) and 1.99 eV for manganese (Zumkley *et al.* 1997). It is in very good agreement with the activation enthalpy of the high-temperature internal-friction mechanism measured by means of mechanical spectroscopy (Feuerbacher *et al.* 1996), where a value of 4.0 eV was found. However, since it has not been clarified yet whether the mechanism of internal friction is associated with dislocation movement, the similarity of the values might be coincidental.

In conclusion, we have presented a detailed description of the dislocation density evolution upon plastic deformation of icosahedral Al–Pd–Mn single quasicrystals. The results show that recovery plays an important role in quasicrystal plasticity. The interpretation of the observed phenomena is in agreement with current models of quasicrystal plastic deformation.

References

Alden, T. H., 1969, *Acta metall.,* **17**, 1435.

Alexander, H., and Haasen, P., 1968, *Solid St. Phys.,* **22**, 27.

Blüher, R., Scharwaechter, P., Frank, W., and Kronmüller, H., 1998, *Phys. Rev. Lett.,* **80**, 1014.

Feuerbacher, M., Baufeld, B., Rosenfeld, R., Bartsch, M., Hanke, G., Beyss, M., Wollgarten, M., Messerschmidt, U., and Urban, K., 1995, *Phil. Mag. Lett.,* **71**, 91.

Feuerbacher, M. Metzmacher C. Wollgarten, M., Urban, K., Baufeld, B., Bartsch, B., and Messerschmidt, U., 1997, *Mater. Sci. Engng.,* **A233**, 103.

Feuerbacher, M., Weller, M., Diehl, J., and Urban, K., 1996, *Phil. Mag. Lett.,* **74**, 81.

Franz, V. Feuerbacher, M., Wollgarten, M., and Urban, K., 1999, *Phil. Mag. Lett.,* **79**, 333.

Geyer, B., Bartsch, M., Feuerbacher, M., Urban, K., and Messerschmidt, U., 2000, *Phil. Mag.* A (in the press).

Gillis, P. P., and Gilman, J. J., 1965, *J. appl. Phys.,* **36**, 3370.

Gottstein, G., 1998, *Physikalische Grundlagen der Metallkunde* (Berlin: Springer).

Ham, R. K., and Sharpe, N. G., 1961, *Phil. Mag.,* **6**, 1193.

Ilschner, B., 1966, *Z. Phys.,* **190**, 258.

Johnston, W. G., 1962, *J. appl. Phys.,* **33**, 2716.

Johnston, W. G., and Gilman, J. J., 1959, *J. appl. Phys.,* **30**, 129.

Kocks, U. F., Argon, A. S., and Ashby, M. F., 1975, *Prog. Mater. Sci.,* **19**,

Li, M. C. J., 1966, *Recrystallization, Grain Growth and Textures* (Metals Park, Ohio: American Society for Metals), p. 45.

Messerschmidt, U., Bartsch, M., Geyer, B., Feuerbacher, M., and Urban, K., 1999, *Phil. Mag.* A, **79**, 2123.

Nordstrom, T. V., and Barrett, C. R., 1972, *J. Mater. Sci.,* **7**, 1052.

Peissker, E., Haasen, P., and Alexander, H., 1962, *Phil. Mag.,* **7**, 1279.

Reid, N. C., Gilbert, A., and Rosenfield, A. R., 1965, *Phil. Mag..,* **12**, 409.

Rosenfeld, R., Feuerbacher, M., Baufeld, B., Bartsch, M., Wollgarten, M. Hanke G. Beyss M., Messerschmidt, U., and Urban, K., 1995, *Phil. Mag. Lett.,* **72**, 375.

Schall, P., 1998, Diploma thesis, Rheinisch–Westfälische Technische Hochschule Aachen.

Seeger, A., 1958, *Handbuch der Physik* (Berlin: Springer), p. 1.
Taylor, G. I., 1934, *Proc. R. Soc.* B, **66**, 362.
Wollgarten, M., Bartsch, M. Messerschmidt, U., Feuerbacher, M., Rosenfeld, R., Beyss, M., and Urban, K., 1995, *Phil. Mag. Lett.,* **71**, 99.
Wollgarten, M., Beyss, M., Urban, K., Liebertz, H., and Köster, U., 1993, *Phys. Rev. Lett.,* **71**, 549.
Yokoyama, Y., Miura, T., Inoue, A., Tsai, A. P., and Masumoto, T., 1992, *Mater. Trans. Japan Inst. Metals,* **33**, 97.
Zumkley, T., Mehrer, H., Freitag, K., Wollgarten, M., Tamura, N., and Urban, K., 1996, *Phys. Rev.* B, **54**, R6815.